IEEE Access
Multidisciplinary | Rapid Review | Open Access Journal

Received March 7, 2019, accepted April 2, 2019, date of publication April 11, 2019, date of current version April 19, 2019.

Digital Object Identifier 10.1109/ACCESS.2019.2910081

Comparison of PD and Breakdown Characteristics Induced by Metal Particles and Bubbles in Flowing Transformer Oil

YONGZE ZHANG[1], JU TANG[1, 2], (Member, IEEE), CHENG PAN[2], (Member, IEEE), AND XINYU LUO[1]

[1]State Key Laboratory of Power Transmission Equipment and System Security and New Technology, School of Electrical Engineering, Chongqing University, Chongqing 400044, China
[2]School of Electrical Engineering, Wuhan University, Wuhan 430072, China

Corresponding author: Cheng Pan (pancheng2036@gmail.com)

This work was supported by the National Natural Science Foundation of China under Grant 51377181.

ABSTRACT Metal particles and bubbles are two typical impurities in transformer oil that can cause partial discharge (PD) and even electric breakdown. The PD characteristics are closely related to the motions of these impurities in flowing transformer oil. In this paper, the motions of impurities were obtained by a camera and a simulation model at first. Then, we employed three methods, namely, antennas, a non-inductive resistor, and the method recommended by IEC 60270, to measure the PD signals simultaneously. The breakdown experiments of transformer oil containing the metal particles and bubbles were also performed. In terms of these, single PD waveforms, statistical characteristics, and breakdown voltage were obtained. The results showed that the metal particles could excite ultrahigh frequency (300 MHz–3 GHz) PD signals, whereas bubbles only excited signals in the very high-frequency band (30–300 MHz). Moreover, the PDs induced by the metal particles had a higher repetition rate and a smaller amplitude than the PDs induced by bubbles. In addition, the metal particles easily caused PD, whereas bubbles easily led to the breakdown. Possible reasons for different discharge characteristics between the two impurities were discussed on the basis of the motions of impurities and the distortions of electric field.

INDEX TERMS Metal particle, bubble, partial discharge, breakdown, flowing transformer oil.

I. INTRODUCTION

A power transformer is one of the most important and expensive equipment in electric power transmission. Specifically, it considerably influences the reliability of the entire power network. Mineral oil impregnated paper is used extensively in transformers as an insulating medium. As the main electrical insulation and heat-eliminating medium, mineral oil directly determines the safe operation of the power transformer. It is a mixture of alkanes, cycloalkanes, and aromatic hydrocarbons that contains many impurities. Although large particles can be removed by oil filter with high vacuum and high precision, the remaining small impurities can agglomerate together to form large particles under a high electrical stress. Some impurity particles can deposit on the surface of transformer tank and parts in manufacturing and assembling. During the operation of transformers, these impurities may fall and mix into the transformer oil due to the vibration of the power transformer or the flushing of oil flow [1]. Other major sources of impurities are insulation aging and failures, such as partial overheating [2], partial discharge (PD) [3]–[5], and spark discharge. Metal particles and bubbles are two typical impurities in transformer oil. As conductive impurities, metal particles can be charged, which have a big threat to transformer insulation. Bubbles can lead to PD due to the low dielectric strength of gas and the high electric field in bubbles.

To study the damage of impurities to the insulation performance of transformer oil, numerous experiments have been conducted [6]–[8]. Bell and Trinh studied the influence of impurities on the breakdown voltage of transformer oil at the early stage. They discovered that impurities can decrease the breakdown voltage, and the larger the impurity

The associate editor coordinating the review of this manuscript and approving it for publication was Bora Onat.

size is, the more evident this effect will be [9], [10]. Pompili conducted PD experiments using a needle-to-plane electrode system and suggested that the first PD may generate bubbles or vapors and the following PD pulse bursts occurred in these bubbles [11]. Moreover, bubble clusters can be generated by Joule heating under the application of pulsed voltage, which can ignite the streamer and then lead to direct ionization in liquid [12]. The size and position of bubbles can affect the PD intensity, and PD tends to occur in large bubbles [13]. Conductive particles are generally the most dangerous impurities. Li focused on the PD characteristics of steel balls with a radius of 1 mm in a quasi-uniform electric field. The author found that the motion of metal balls could be divided into oscillating and jumping stages, which directly affected the PD behavior [14]. Sarathi focused on the PD induced by an aluminum ball with a radius of 1.25 mm. The result showed that the PD induced by large metal balls could excite ultrahigh frequency (UHF) signals with frequency contents of 0.5 GHz to 1.2 GHz and 1 GHz to 3 GHz under AC and DC conditions, respectively [15].

Previous studies have usually focused on one type of impurity, either bubbles or metal particles. However, comparing their discharge characteristics is difficult due to differences in test condition. The ambiguity of the discharge characteristics is not conducive for detecting the PD in the actual transformer nor for clarifying the breakdown mechanism of transformer oil contaminated by impurities. Moreover, previous investigations have mostly focused on stationary transformer oil; however, the oil moves in a large running transformer due to various cooling systems. Therefore, studies on flowing transformer oil are important for engineering applications. Our research team recently investigated the effect of oil velocity on PD activities induced by bubbles and metal particles [16], [17]. We found remarkable differences between PD activities in flowing and stationary states. Particularly, PD activities further become weak as oil velocity increases. This finding is consistent with the research of Li *et al.* [18]. Hence, all experiments in the present paper were conducted on the basis of flowing transformer oil.

In the present work, we aim to clarify different characteristics of PD and breakdown induced by metal particles and bubbles in flowing transformer oil. PD and breakdown experiments were performed on an experimental platform of flowing transformer oil. We adopted several methods to measure PD signals and obtained single PD waveforms and phase resolved PD (PRPD) patterns. Then, we summarized the different effects of the two types of impurity on the insulation performance of transformer oil. Finally, we explained the different discharge characteristics on the basis of the motions of impurities and electric field analysis.

II. EXPERIMENTAL SETUP AND METHOD

A. EXPERIMENTAL SETUP

To perform PD and breakdown experiments, we established an experimental platform of flowing transformer oil [17], as shown in Fig. 1. The main oil duct was composed of

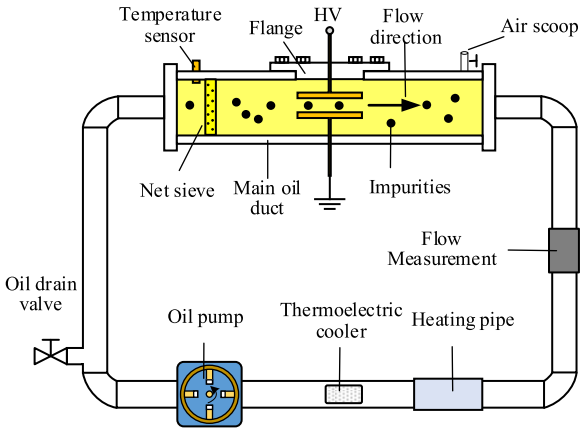

FIGURE 1. Circulation device of flowing transformer oil for PD and breakdown experiments.

polymethyl methacrylate, which is a transparent lightweight insulation material. We designed two flat plate electrodes with a diameter of 200 mm and a thickness of 10 mm to create a uniform electric field. The distance between the two electrodes was 10 mm. A flange above the main oil duct was prepared for the changes of electrodes and impurities. We used a net sieve with 3 mm openings to limit the diameter of bubbles below 3 mm. The temperature of the entire device was controlled using a temperature sensor, thermoelectric cooler, and heating pipe. Oil circulation was achieved with an oil pump. Generally, oil velocity is lower than 0.5 m/s in the actual transformer, and most transformers operate in the range of 40 °C to 80 °C [19], [20]. Hence, all of the experiments were conducted at a velocity of 0.30 m/s in the main oil duct and temperature of 60 °C.

B. MEASUREMENT METHOD

We used several methods in detecting PD signals to investigate fully the differences between PDs induced by bubbles and metal particles. First, a noninductive resistor was utilized to obtain the PD current pulses, which were closer to the real discharge current waveforms. Second, two types of antenna were used to measure the electromagnetic radiation of PD due to their wide application in online monitoring. One type was a microstrip patch antenna with a center frequency of 390 MHz and a bandwidth of 340 MHz to 440 MHz (UHF antenna), which has been applied to online monitoring. The other type was a sleeve monopole antenna with a center frequency of 100 MHz and a bandwidth of 20 MHz to 250 MHz (very high frequency (VHF) antenna). Although the two antennas do not cover all frequency bands of VHF and UHF, they can effectively reveal the differences in the electromagnetic radiation signals of PD induced by metal particles and bubbles. However, the antenna method cannot completely determine the amount of charge. Hence, the conventional measurement method recommended by IEC 60270 was also adopted [21]. The PD waveform obtained by the conventional method is completely different from the real discharge

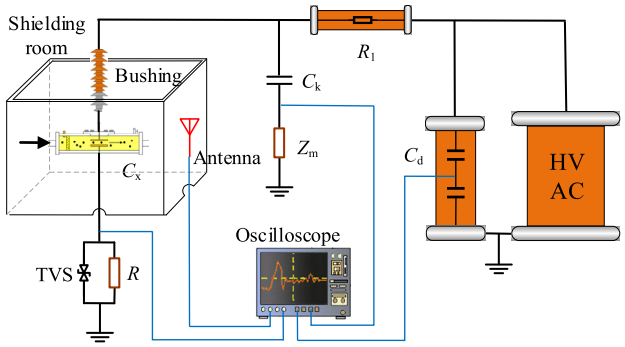

FIGURE 2. Experimental circuit and measurement system.

current waveforms. Thus, this method was only used to determine the amount of charge and repetition rate. Fig. 2 shows the experimental measurement system. The circulation device C_x was placed in a shielding room. R_1 was a protection resistor. The measuring circuit recommended by IEC 60270 comprised an impedance detector Z_m and a coupling capacitor C_k. PD signals detected by Z_m were set as the trigger signals for oscilloscope (DPO 7104). A transient voltage suppressor (TVS), which was connected in parallel to a 50Ω noninductive resistor R, could protect the oscilloscope from overloading when a breakdown occurred accidentally. The signals measured by the antenna (VHF or UHF), the noninductive resistor R, the impedance detector Z_m, and the capacity voltage divider C_d were synchronously inputted into the oscilloscope.

Before test, the mineral oil (Karamay No. 25) was filtered to remove impurities larger than 5 μm in diameter. Then, the oil was carefully dried and degassed with a vacuum degassing and dehydration system. The breakdown voltage of the processed transformer oil was 75 kV according to the procedure and the cell-container described in IEC 60156 [22], which reached the engineering application requirements. To avoid the PD disturbances from high-voltage lines, the maximum of the allowable applied voltage of the following PD tests was measured. The oil duct was filled with processed oil (without any artificial insulation defect). PD disturbances occurred when the voltage rose to 35 kV. Hence, if the applied voltage of following PD experiments was below 35 kV, the experiment results were free of disturbances from high-voltage lines.

In an actual transformer oil, the diameter of metal particles ranges from 5 μm to 200μm [7]. Large particles generally cause more serious harm to oil insulation than smaller ones; thus, the diameter of particles was set to 150μm. The concentration of metal particles was set to 1.0 g/L [23]. In the bubble experiments, 250 mL dry air was injected into the oil duct through the air scoop. The air mass was broken into small bubbles by the oil pump, and the net sieve controlled the diameter of bubbles below 3 mm [24].

III. MOTIONS OF IMPURITIES

Small metal particles and bubbles can move with oil flow in an actual transformer. Their motions can affect the characteristics of PD and breakdown [25]. We used a camera to capture the motions of bubbles. However, it is quite difficult to capture the motions of metal particles because the size of particles is greatly smaller than that of the oil duct. Thus, we constructed a physical mode involving multiple forces to simulate the motions of metal particles.

A. MOTIONS OF BUBBLES

The motions of bubbles are dominated by buoyancy, oil drag force, pressure gradient force, Maxwell stress tensor, and surface tension. The motions were recorded by a video camera that was operated at 120 frames s^{-1}. Fig. 3 shows the motions of small and large bubbles at the applied voltage of 10 kV.

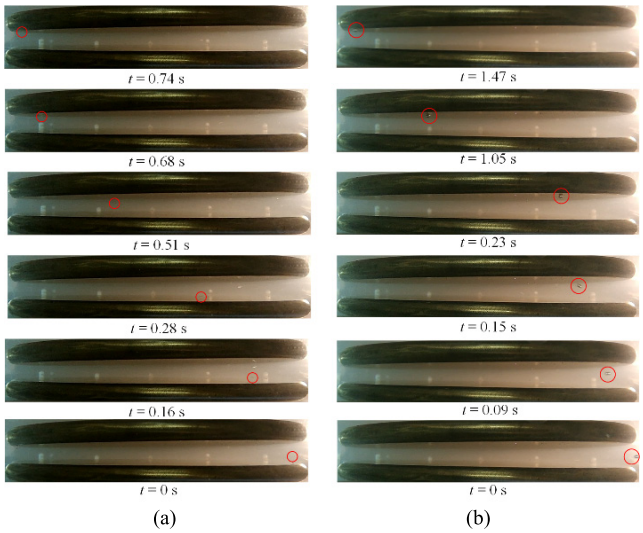

FIGURE 3. Motions of bubbles with diameters of (a) 0.8 mm and (b) 2.0 mm.

As shown in Fig. 3, bubbles gradually approached the top electrode while moving in the direction of oil flow. The large bubble (diameter of 2.0 mm) reached the upper electrode at $t = 0.23$ s, whereas the small bubble (diameter of 0.8 mm) did not reached the upper electrode until $t = 0.74$ s. Hence, the large bubble was mainly distributed near the upper electrode, and the small bubble was mainly distributed in the oil bulk. Besides, the large bubble required longer time to pass through the electrode than the small bubble did due to the viscidity of liquid. The viscidity function slows the oil velocity near the electrode, and the velocity in the central region is the largest. Therefore, the velocity of the large bubble (near the electrodes) was low, whereas that of the small bubble (in the oil bulk) was high. The position and duration of bubbles in the high electric field may further affect the PD and breakdown characteristics.

B. MOTIONS OF METAL PARTICLES

As conductive impurities, metal particles can be charged by contacting with electrodes; hence, the Coulomb force plays an important role in the movement of metal particles. The motion equation of charged metal particles can be

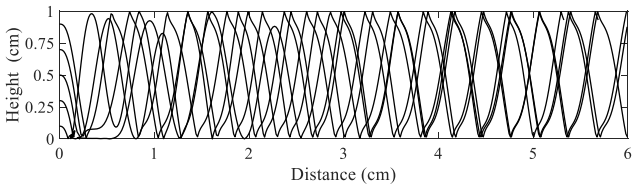

FIGURE 4. Trajectories of metal particles.

expressed as

$$\frac{4}{3}\pi r_{\mathrm{p}}^3 \rho_{\mathrm{p}} \frac{du_{\mathrm{p}}}{dt} = F_{\mathrm{drag}} + F_{\mathrm{e}} + F_{\mathrm{g}} + F_{\mathrm{other}}, \tag{1}$$

where r_{p} is the radius of the particles, and ρ_{p} is density of metal particles (set as 7850 kg/m^3).

Both sides of (1) are the resultant force of metal particles. The oil drag force F_{drag} [26], the electric field force F_{e} [27], and the force F_{g} caused by the gravity and different densities can be expressed as follows:

$$F_{\mathrm{drag}} = \frac{1}{2} C_{\mathrm{d}} \pi r_{\mathrm{p}}^2 \rho_1 \left(u_1 - u_{\mathrm{p}}\right) \left|u_1 - u_{\mathrm{p}}\right|, \tag{2}$$

$$F_{\mathrm{e}} = \frac{2}{3} k \pi^3 r_{\mathrm{p}}^2 \varepsilon_{\mathrm{r}} \varepsilon_0 E^2 \sin(\omega t + \theta) \sin(\theta), \tag{3}$$

$$F_{\mathrm{g}} = \frac{4}{3} \pi r_p^3 g \left(\rho_{\mathrm{p}} - \rho_1\right), \tag{4}$$

where C_d is the drag coefficient; u_p is the velocity of the transformer oil; k is the correction coefficient related to the image charge, which is recommend as 0.83 [28]; ε_{r} is the relative permittivity of the transformer oil (set as 2.2); ε is the permittivity of free space; E is the uniform electric field; θ indicates the phase of metal particles leaving the electrode; and ρ_l is the density of the transformer oil (set as 850 kg/m^3).

F_{other} includes Saffman force F_{S}, Magnus lift force F_{M}, pressure gradient force F_{P}, Basset force F_B, and additional mass inertia force F_{VM}, as shown in (5). F_{other} is considerably lower than F_{drag}, F_{e}, and F_{g}; thus, it can be neglected [26]. The motion in the vertical direction of metal particles is determined by F_{e} and F_{g}. The direction of F_{drag} is related to the oil velocity and particle velocity. Hence, F_{drag} can affect the vertical and horizontal motions.

$$F_{\mathrm{other}} = F_{\mathrm{S}} + F_{\mathrm{M}} + F_{\mathrm{P}} + F_{\mathrm{B}} + F_{\mathrm{VM}} \tag{5}$$

Fig. 4 plots the trajectories of metal particles with a diameter of 150 μm under an AC voltage of 10 kV and a velocity of 0.30 m/s. Metal particles moved back and forth between the two electrodes while moving horizontally with the oil flow. The repeated collisions with two electrodes were similar to the report in [29]. The motion of metal particles was completely different from that of bubbles. The variations in conductivity, volume, and density of the two impurities result in the completely different motions that also have various effects on the insulating properties of the transformer oil.

IV. RESULTS

A. PD INCEPTION VOLTAGE

We continuously increased the applied voltage to the PD occurrence (PD $\geq$ 100 pC) at a rate of 1 kV/s to obtain the partial discharge inception voltage (PDIV) in accordance with IEC 61294 [30]. The PDIV measurements were repeated 10 times because PD has a stochastic nature in principle. The average PDIVs of metal particles and bubbles in transformer oil were 8.4 kV and 23.2 kV, respectively, as Fig. 5. The PDIV of bubbles was higher than that of metal particles. The test voltage of PD experiments was set to 1.2 times the PDIV. Hence, the applied voltages were set as 10.0 kV and 27.9 kV in the following PD tests of metal particles and bubbles, respectively.

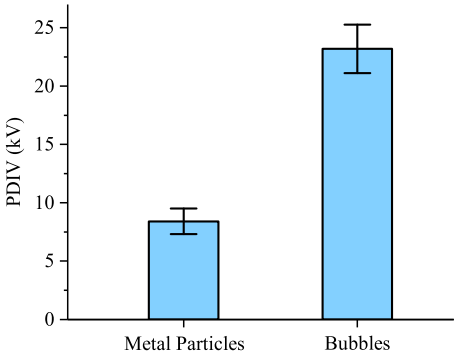

FIGURE 5. The average PDIVs of metal particles and bubbles.

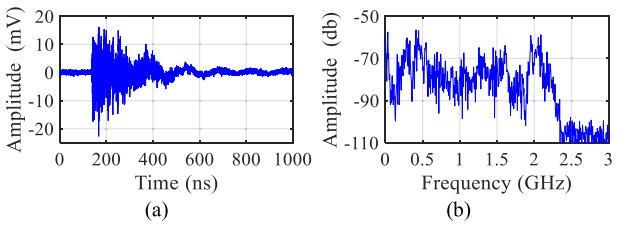

FIGURE 6. (a) Electromagnetic radiation signals of metal particles and (b) FFT analysis.

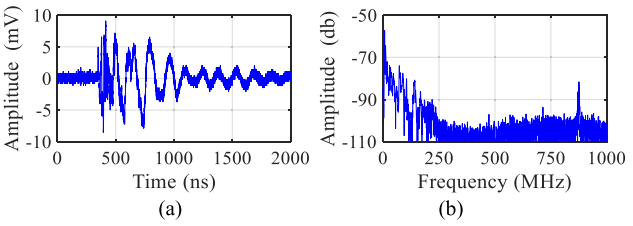

FIGURE 7. (a) Electromagnetic radiation signals of bubbles and (b) FFT analysis.

B. PD SIGNALS MEASURED BY ANTENNAS

Fig. 6 shows the typical PD signal measured by the UHF antenna and fast Fourier transformation (FFT) analysis from metal particles. Fig. 7 plots the typical bubble-induced PD signal measured by the VHF antenna and FFT analysis. We identified remarkable distinctions between the two signals. The oscillation frequency and amplitude of PD induced by metal particles were higher than those induced by bubbles. The durations of the signal induced by metal particles and

TABLE 1. Characteristic parameters of current pulses (ns).

Parameter	Metal particles	Bubbles
t_r	3.1	25.1
t_d	2.4	20.9
t_w	4.4	41.1

bubbles were approximately 250 ns and 700 ns, respectively. The frequency content of PD induced by metal particles was in the range of 300 MHz to 2.3 GHz (in the UHF range), whereas that of bubble-induced PD was below 200 MHz (in the VHF range). Although the excitation mechanism of electromagnetic signals is not completely clear at present, electromagnetic signal is generally related to the short rise time of current pulse [31]. Therefore, we further measured the current pulses by a 50 Ω noninductive resistor, which will be discussed in the next section.

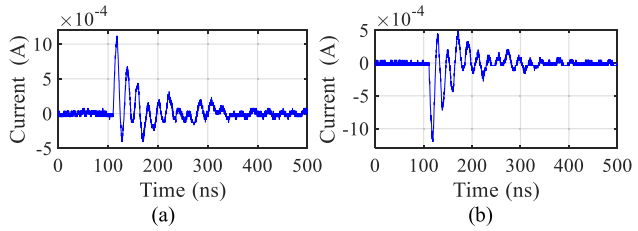

FIGURE 8. Current pulses of metal particles measured by *R*: (a) positive, (b) negative.

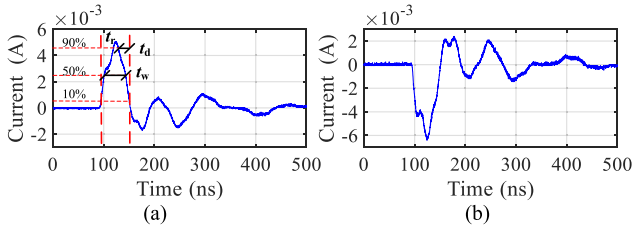

FIGURE 9. Current pulses of bubbles measured by *R*: (a) positive, (b) negative.

C. PD CURRENT PULSES MEASURED BY NONINDUCTIVE RESISTOR

Figs. 8 and 9 show the typical positive and negative current pulses of metal particles and bubbles measured by R, respectively. We extracted 90% rise time t_r, 90% fall time t_d, and 50% amplitude pulse duration t_w to quantitatively compare the current pulses induced by the two impurities, which are also illustrated in Fig. 9a. The average results of 100 PD current pulses are shown in Table 1.

Thet_r of the current pulse of metal particle-induced PD and of bubble-induced PD were only 3.1 ns and 25.1 ns, respectively. As shown in Table 1, the t_r, t_d, and t_w of metal particles were shorter than those of bubbles. The durations of the PD current pulses induced by metal particles and bubbles were approximately 150 ns and 250 ns, respectively. Moreover, the oscillation of the current pulse of metal particles was considerably more severe than that of bubbles. The waveforms of positive and negative current pulse were similar, except for the opposite polarity.

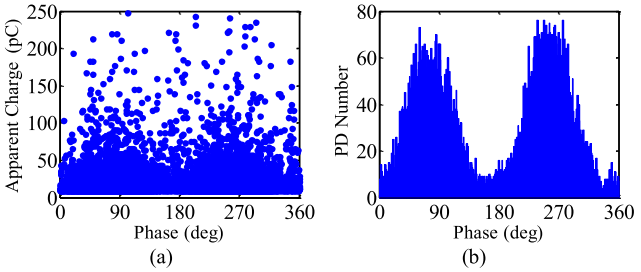

FIGURE 10. PRPD patterns of metal particles: (a) φ–q, (b) φ–n.

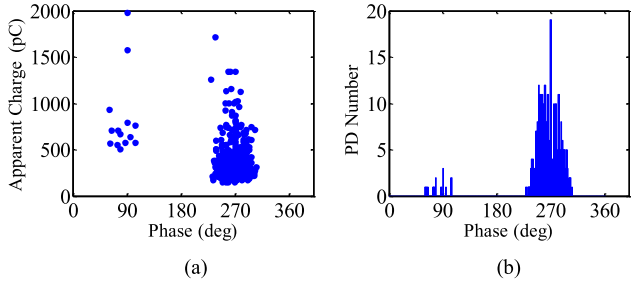

FIGURE 11. PRPD patterns of bubbles: (a) φ–q, (b) φ–n.

D. PRPD PATTERNS

The distribution of bubbles and metal particles has strong randomness, and PD signals have obvious randomness in amplitude and phase. Thus, a single PD cannot represent the PD characteristics. We conducted continuous PD experiments for 30 minutes to reveal the differences between PDs induced by the two impurities. The discharge phase φ, apparent charge q, and the number of PDs n were extracted on the basis of the PD signals measured by the conventional method. The amplitude of the PD occurring in the negative half-cycle is negative. To clearly compare the magnitudes of PDs occurring in the positive and negative half-cycles, the following apparent charges were replaced by their absolute values. PD experiments of each impurity were repeated five times. The results of the five experiments were consistent. As such, the experiments had good repeatability. Figs. 10 and 11 show the PRPD patterns of metal particles and bubbles, respectively.

We observed remarkable differences in PRPD patterns of the two impurities. For metal particles, PDs almost occupied the entire power frequency cycle. The graphs of positive and negative half-circles were similar. For bubble-induced PD, all the discharges were distributed in the range of 60° to 104° and 236° to 305°. The phase with the largest number of PDs was 270°. Most PDs occurred in the negative half-cycle, and the polarity effect was evident. The comparison of Figs. 9 and 10 showed that although the apparent charge of PD

induced by metal particles was small, its frequency was high. By contrast, although the apparent charge of bubble-induced PD was large, its frequency was low. To show the differences clearly, we further extracted statistical characteristics, namely, the pulse repetition rate, average apparent charge, and accumulated apparent charge in unit time, which will be discussed in the next section.

E. PD STATISTICAL CHARACTERISTICS

The number of PDs occurring in positive and negative half-cycles and the total number of PDs were recorded as $N+$, $N-$, and N, respectively. We defined the unit time as 1 minute. Thus, the number of PDs was converted to pulse repetition rate in 1 minute. The results are shown in Table 2. The pulse repetition rates N of metal particles and of bubbles were 394.43 and 13.70 per minute, respectively. The pulse repetition of metal particles was extremely higher than that of bubbles. No considerable difference was observed between the $N+$ and $N-$ of PD induced by metal particles. However, the $N-$ of bubble-induced PD was greatly higher than the $N+$.

TABLE 2. Pulse repetition rate (per minute).

Parameter	Metal particles	Bubbles
N-	204.37	13.23
N+	190.06	0.47
N	394.43	13.70

Average apparent charge is the ratio of the total PD apparent charge to the number of PDs. The average apparent charge of PD that occurred in the positive half-cycle, negative half-cycle, and the total average apparent charge were recorded as $Q_{ave}+$, $Q_{ave}-$, and Q_{ave}, respectively. The results are shown in Table 3.

TABLE 3. Average apparent charge (pC).

Parameter	Metal particles	Bubbles
Q_{ave-}	52.97	387.56
Q_{ave+}	51.62	825.41
Q_{ave}	52.31	402.58

Given the two preceding characteristic parameters, PD induced by metal particles had high repetition rate, whereas bubble-induced PD had high apparent charge. In view of the PD intensity, the repetition pulse only covers the PD frequency; however, it lacks information on amplitude. Moreover, the average apparent charge lacks information on frequency. Hence, the accumulated apparent charge in unit time (1 minute) was calculated. It contains frequency and amplitude information. The accumulated apparent charge was recorded as Q_{acc}, and Q_{acc+} and Q_{acc-} for positive and negative half-cycles, respectively. The results are shown in Table 4. From the table, the accumulated apparent charge of metal particles was considerably higher than that of bubbles, and the PD intensity of metal particles was more severe than that of bubbles.

TABLE 4. Accumulated apparent charge (pC).

Parameter	Metal particles	Bubbles
Q_{acc-}	10825.48	5127.42
Q_{acc+}	9810.90	387.94
Q_{acc}	20636.38	5515.36

F. BREAKDOWN VOLTAGE

Breakdown voltage is an important parameter that can evaluate the effects of bubbles and metal particles on the insulation performance of transformer oil. The experiment conditions were the same as PD tests. The applied voltage was continuously increased to breakdown at a rate of 2 kV/s. Breakdown experiments were repeated 10 times. The average breakdown voltage of the 10 experiments of flowing transformer oil with metal particles and bubbles were 42.0 kV and 31.6 kV, respectively. Their relative standard deviations were 4.5% and 6.2%, respectively. The bubbles had a substantial influence on the decrease in breakdown voltage.

V. DISCUSSIONS

A. PDIV

The PDIV of metal particles was considerably lower than that of bubbles; thus, metal particles can easily cause PD. This phenomenon may be related to the discharge mechanism determined by the nature of the two impurities.

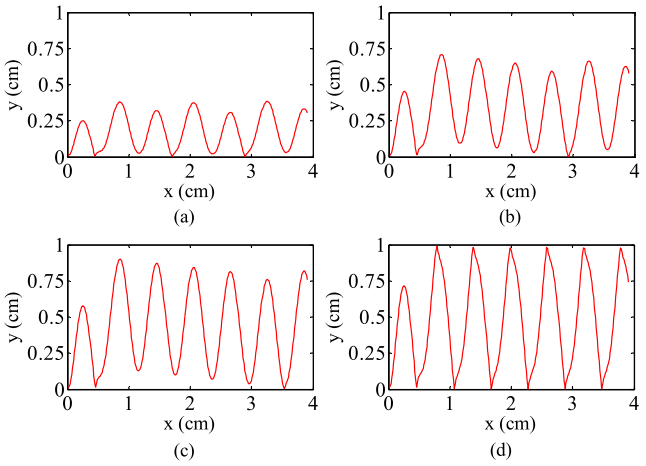

FIGURE 12. Motions of metal particles under different applied voltages. (a) 6 kV. (b) 8 kV. (c) 9 kV. (d) 10 kV.

Sarathi found that PD incepted when the spherical particle jumped from one electrode to another [32]. The motion of metal particles was determined by the applied voltage. Therefore, the PDIV of metal particles could be estimated on the basis of the particle movement. We simulated the motions of the metal particles under different applied voltages using the previous model. The results are shown in Fig. 12.

When the applied voltage was 6 kV, the metal particle moved near the ground electrode because of the limitation of alternating voltage, as Fig. 12a. The jumping height of the particle increased with the applied voltage due to the increase of Coulomb force. When the applied voltage reached 10 kV, the charged metal particle regularly collided with the two electrodes, which meant the PD inception. Therefore, the calculated PDIV of metal particles was 10 kV. The initial position of the metal particles was on the surface of the ground electrode in this simulation. Some charged metal particles were suspended in the transformer oil and could easily collide with the two electrodes, as shown in Fig. 4. Therefore, the PDIV of metal particles should be lower than 10 kV. The experimental measurement was 8.4 kV, which was in agreement with the simulations.

The PD induced by bubbles is the breakdown progress in bubbles. Therefore, we can estimate the PDIV of the transformer oil containing bubbles based on the breakdown strength of the bubble. Since the bubble diameter was limited to less than 3 mm and the electric field in bubbles was uniform, Paschen's law is available here. The breakdown strength E_b of bubbles derived from Paschen's law are expressed as follows [33]:

$$E_b = \frac{Bp}{\ln(pd) + k}, \tag{6}$$

where constant B is 2737.5 V/kPa · cm, p is the pressure, d is the diameter of bubbles, and k can be expressed as

$$k = 3.5134(\mathrm{pd})^{0.05999}, \tag{7}$$

when pd is in the range of 0.2 to100 kPa·cm. The change of E_b with the bubble diameter can be obtained by (6) and (7), as Fig. 13. Fig. 13 shows that E_b declines with the increase of bubble diameter. On the other hand, the electric field strength inside the bubbles of different sizes is almost equal. Therefore, PD first occurs in large bubbles. Hence, we only focused on the E_b of the bubble with a diameter of 3 mm, which was as low as 35.81 kV/cm.

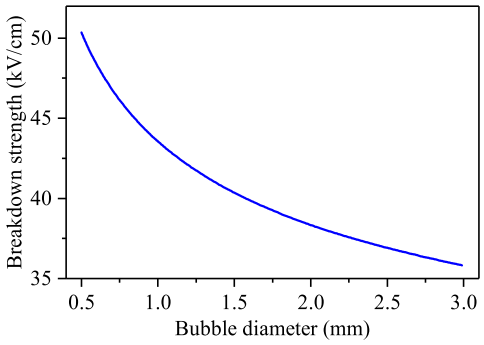

FIGURE 13. Change of E_b with the bubble diameter.

To determine the applied voltage on the electrodes by the E_b (35.81 kV/cm), we performed electrostatic field simulation. The deformation of the bubble was ignored for simplicity. As shown in Fig. 14, the electric field in bubbles

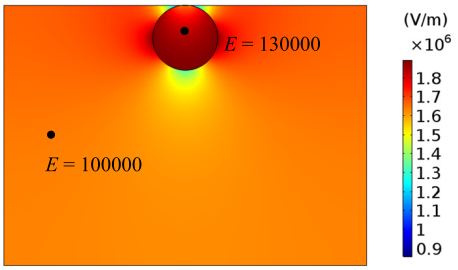

FIGURE 14. Electric field distribution in transformer oil containing a bubble with applied voltage of 1 kV and distance of 1 cm.

was 1.30 times that in transformer oil. Therefore, the peak value of the applied voltage between the two electrodes was 27.55 kV. Accordingly, the calculated effective voltage was 19.48 kV. The experimental PDIV was 23.2 kV, which was larger than the calculation. The deviation may arise from several reasons. First, the applied voltage was alternating, so PD may not occur until the electric field in bubbles was higher than E_b for a period. Second, the effect of space charge was not considered, which resulted in the actual electric field in bubbles being slightly lower than the calculation. Then, the actual bubble size may be smaller than 3 mm, which also enhanced the experimental PDIV.

B. PD WAVEFORM

Electromagnetic radiation signals measured by antennas and current pulses measured by noninductive resistor showed obvious differences in PDs between the metal particles and bubbles. As shown in Figs. 5 and 6, PD induced by metal particles could excite UHF signals, whereas bubble-induced PD could only excite VHF signals. In accordance with the measurement of noninductive resistor, the rise time of the current pulse induced by metal particles and bubbles were 3.1 ns and 25.1 ns, respectively. Some researchers have proposed that short PD current pulses had more spectral energy at high frequencies [31]. Therefore, the short rise time of the current pulse is responsible for the UHF PD signals induced by metal particles. Hence, the measurements of current pulses are in agreement with the electromagnetic radiation signals. Next, we explain the reasons for the differences between the rise time of the two types of PD via theoretical calculation.

The rise time of current pulse corresponds to the propagation time of streamer [34], [35]. The propagation time of the streamer induced by metal particles is determined by the discharge gap and the propagation speed. Initially, we calculated the discharge gap. Birlasekaran discovered that microdischarges occur when the electric field reaches 70 MV/m [36].

The electric field distortion changes with the distance between the metal particles and the electrode. Before calculating the changes of electric field with distance, we initially calculated the amount of charge of metal particles. The metal particles had the same potential with the electrode after colliding with it [37]. Therefore, the amount of charge of the

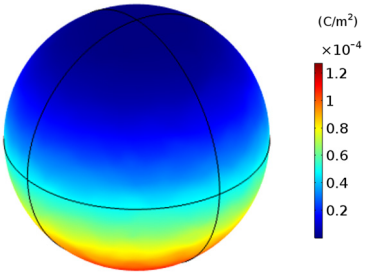

FIGURE 15. Surface charge density of the charged metal particle.

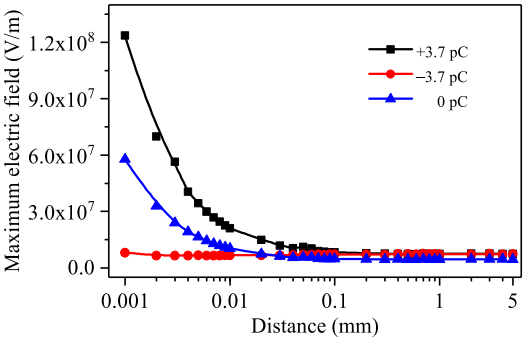

FIGURE 16. Changes of the maximum electric field with the distances between the metal particles and the upper electrode.

metal particles could be obtained according to the potential. An extreme case was considered, in which the potential of high voltage electrode was at peak value for simplicity. The surface charge density of the metal particles with a diameter of 150 μm is shown in Fig. 15 under the applied voltage of $10 \times \sqrt{2}$ kV. The total charge of the metal ball equaled to 3.7 pC, which was calculated by integrating the surface charge density along the spherical surface. Birlasekaran also proposed a formula for calculating the charge of metal particles, as shown in (8) [27].

$$q = \frac{2}{3}\pi^3 r_p^2 \varepsilon_r \varepsilon_0 E \tag{8}$$

In accordance with (8), the charge q of metal particles was 3.2 pC, which was nearly equal to the simulation result in the present work, thereby proving the accuracy of the simulation. We set the upper electrode as kV in the simulation model of electrostatic field. The charges of metal particles were set as 3.7, −3.7, and 0 pC. Fig. 16 shows the changes of the maximum electric field with the distance between the metal particles and the upper electrode. When the polarities of metal particles and the electrode were opposite, the distortion of electric field was the most serious. For ground electrodes, the influence of distance and polarity on electric field distortion were the same as that of the upper electrode. We only considered the case of opposite polarity for simplicity. The closer the particle was to the electrode, the more severe the electric field distortion was. When the distance was 2 μm, the maximum electric field in oil reached 70 MV/m. Therefore, the discharge gap was approximately 2 μm. The next step is to obtain the streamer velocity.

Wang *et al.* found that the velocity of a streamer was approximately 1.5 km/s by a high-speed video [38]. Thus, the propagation time of the streamer induced by metal particles was 1.33 ns in accordance with the discharge gap and the velocity. The theoretical result was slightly less than the experimental measurement. This deviation may be caused by the response delay of the measure system. The short current pulses induced by metal particles that occurred in the transformer oil excited the UHF PD signals.

The PD induced by bubbles occurs in bubbles. Therefore, the propagation time of streamer was determined by the size of the bubbles and the propagation speed of the streamer in the air. Fig. 13 shows that PD tends to occur in large bubbles. The bubble diameter was limited to less than 3 mm in the present word. Briels *et al.* found that the average speed of the streamer was approximately 0.123 mm/ns [39]. Thus, the propagation time of the streamer induced by bubbles was 24.39 ns, which is close to the measurement. The rise time of current pulses was slow. Hence, PD induced by bubbles only excited VHF signals.

UHF antennas have been used for online monitoring of power transformers. However, this technology cannot find PD induced by bubbles, as verified by the experiments. The presence of bubbles easily resulted in the breakdown of the complete oil gap. Therefore, monitoring of bubbles should be further studied.

C. PRPD PATTERNS

The phase distribution of metal particle-induced PD nearly covered the entire power frequency cycle, and the PRPD patterns in the positive and the negative half-cycles were symmetrical. The wide phase distribution of metal particle-induced PD may be due to the randomness of collisions. As shown in Fig. 4, the initial positions could affect the particle trajectories, thereby further changing the PD phase.

In comparison with the PD induced by metal particles, the phase distribution of bubble-induced PD was relatively narrow. As previously mentioned, bubble-induced PD is the breakdown of bubbles. PD would not occur until the electric field in bubbles exceeds E_b. In the PD experiments of bubbles, the applied voltage was 27.9 kV. Thus, the phases exceeding the E_b of bubbles with a diameter of 3 mm (35.81 kV/cm) were in the range of 65° to 115° and 245° to 295°. The experiment measurement was in the range of 60° to 104° and 236° to 305° . Therefore, the calculations agree with the measurements. Besides, the narrow phase distribution may be responsible for the low pulse repetition rate of bubbles.

Another considerable difference was the φ–n pattern between the two types of PD. The φ–n patterns of metal particles were symmetrical, whereas those of bubble-induced PD were concentrated in the negative half-cycle. PD occurs when metal particles collide with the opposite electrode. Therefore, we counted the number of collisions in the positive

and negative half-cycles in Fig. 4, which were 43 and 44, respectively. Hence, the φ–n patterns of metal particles were symmetrical, and the numbers of PDs in the negative and positive half-cycles were almost equal. Frequent collisions were also responsible for the high repetition rate of PD induced by metal particles. Then, the high repetition rate led to the high accumulated apparent charge of metal particles shown in Table 4.

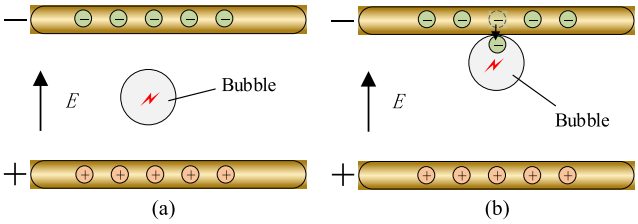

FIGURE 17. Different types of bubble: (a) isolated bubble; (b) boundary bubble.

The polarity effect of bubble-induced PD may be related to the sources of seed electrons, which associate with the location of the bubbles. The motions of bubbles (Fig. 3) indicated that bubbles either existed in the oil bulk (defined as isolated bubbles) or near the upper electrode (defined as boundary bubbles) [11], as shown in Fig. 17. For isolated bubbles, the polarity of the applied voltage has no effect on PD induced by isolated bubbles because the different polarities only indicate the exchange of electrode positions. If only for this case, then the φ–q and φ–n patterns should be symmetrical. However, the experiment results showed obvious polarity effect. There should be another situation, in which PD easily occurs in the negative half-cycle. This type might be the PD induced by boundary bubbles. Fig. 3 shows that large bubbles are mainly distributed near the upper electrode and take longer to pass through the two electrodes, which mean that boundary bubbles stay longer in electric field and their size is large. Furthermore, large bubbles are more likely to cause PD, as depicted in Fig. 13. The interface of boundary bubbles directly connects with the metal electrode, which can provide additional sources of free electrons in the negative half-cycle. Therefore, most PDs induced by bubbles occurred in negative half-cycles.

D. BREAKDOWN VOLTAGE

The breakdown voltages of flowing transformer oil containing metal particles and bubbles were 42.0 kV and 31.6 kV, respectively, at the same oil gap in this experimental condition. The presence of bubbles had a considerable effect on the decrease in breakdown voltage. The phenomena may be related to the high average apparent charge of bubble-induced PD (Table 3). The higher the apparent charge, the more severe the local overheating. Then, local overheating causes the expansion of bubbles and the further decomposition of liquid, thereby producing additional gas. The streamer propagates with the development of the gas channel [40], [41]. Breakdown occurs when the streamer connects the upper and lower electrodes. In addition to the high average apparent charge, bubbles can directly participate in the process of streamer propagation, which also contributes to the low breakdown voltage of transformer oil containing bubbles.

Although the PD intensity induced by bubbles was smaller than that of metal particles (Table 4), the breakdown voltage of transformer oil containing bubbles was lower than that of metal particles, which suggests that bubbles also pose a great threat to transformer insulation. Hence, it is important to first identify the type of defect in assessing the effect of insulation defects on the insulation performance of transformer on the basis of PD intensity.

VI. CONCLUSIONS

In this study, we obtained the motions of metal particles and bubbles in flowing transformer oil. PD and breakdown experiments in flowing transformer were performed. The effects of the two impurities on the insulation performance of transformer oil was analyzed on the basis of their motions and the distortion of electric field. The results showed that the PDIV of metal particles was considerably lower than that of bubbles. PD induced by metal particles had high pulse repetition rate and small apparent charge, whereas PD induced by bubbles had low pulse repetition rate and large apparent charge. The PRPD patterns of metal particles were symmetrical, whereas those of bubbles had remarkable polarity effect, which may be used for fault identification in the future.

The PD current pulses induced by metal particles had a shorter rise time and a severe oscillation, which could excite UHF signals. By contrast, the current pulses induced by bubbles had a longer rise time and a weaker oscillation, and they could not excite UHF signals. Therefore, as an online monitoring approach, the UHF method could not detect bubble-induced PDs. In addition, the breakdown voltage of flowing transformer oil contaminated by bubbles was considerably lower than that of metal particles. Thus, the bubble detection should be given further attention.

The oil flow in an actual transformer is relatively complicated. Thus, oil flows in horizontal and vertical directions. The flow direction directly affects the motions of impurities and discharge characteristics. For future studies, vertical oil flow direction should be considered.

REFERENCES

[1] M. Bagheri, A. Zollanvari, and S. Nezhivenko, "Transformer fault condition prognosis using vibration signals over cloud environment," *IEEE Access*, vol. 6, pp. 9862–9874, 2018.
[2] M. Tsuchie, M. Kozako, M. Hikita, and E. Sasaki, "Modeling of early stage partial discharge and overheating degradation of paper-oil insulation," *IEEE Trans. Dielectr. Electr. Insul.*, vol. 21, no. 3, pp. 1342–1349, Jun. 2014.
[3] X. Chen, Y. Qian, Y. Xu, G. Sheng, and X. Jiang, "Energy estimation of partial discharge pulse signals based on noise parameters," *IEEE Access*, vol. 4, pp. 10270–10279, 2016.
[4] J. Tang *et al.*, "Investigation of partial discharge between moving charged metal particles and electrodes in insulating oil under flow state and AC condition," *IEEE Trans. Dielectr. Electr. Insul.*, vol. 23, no. 2, pp. 1099–1105, Apr. 2016.

[5] L. Luo, B. Han, J. Chen, G. Sheng, and X. Jiang, "Partial discharge detection and recognition in random matrix theory paradigm," *IEEE Access*, vol. 5, pp. 8205–8213, 2016.

[6] A. Denat, F. Jomni, F. Aitken, and N. Bonifaci, "Thermally and electrically induced bubbles in liquid argon and nitrogen," *IEEE Trans. Dielectr. Electr. Insul.*, vol. 9, no. 1, pp. 17–22, Feb. 2002.

[7] X. Wang and Z. D. Wang, "Particle effect on breakdown voltage of mineral and ester based transformer oils," in *Proc. Annu. Rep. Conf. Electrl. Insul. Dielectr. Phenom.*, Quebec, QC, Canada, Oct. 2008, pp. 598–602.

[8] R. Sarathi, A. V. Giridhar, A. Mani, and K. Sethupathi, "Investigation of partial discharge activity of conducting particles in liquid nitrogen under DC voltages using UHF technique," *IEEE Trans. Dielectr. Electr. Insul.*, vol. 15, no. 3, pp. 655–662, Jun. 2008.

[9] W. R. Bell and M. Danikas, "Factors affecting the breakdown strength of transformer oil," in *Proc. IEEE Int. Conf. Electr. Insul.*, Philadelphia, PA, USA, Jun. 1982, pp. 264–267.

[10] N. G. Trinh, R. Olivier, C. Vincent, and J. Regis, "Effect of impurity particles on transformer oil under normal operating conditions," in *Proc. IEEE Int. Conf. Electr. Insul.*, Boston, MA, USA, Jun. 1980, pp. 225–228.

[11] M. Pompili, C. Mazzetti, and E. O. Forster, "Partial discharge distributions in liquid dielectrics," *IEEE Trans. Electr. Insul.*, vol. 27, no. 1, pp. 99–105, Feb. 1992.

[12] H. Fujita, S. Kanazawa, K. Ohtani, A. Komiya, T. Kaneko, and T. Sato, "Initiation process and propagation mechanism of positive streamer discharge in water," *J. Appl. Phys.*, vol. 116, no. 21, Dec. 2014, Art. no. 213301.

[13] H. Shiota, H. Muto, H. Fujii, and N. Hosokawa, "Diagnosis for oil-immersed insulation using partial discharge due to bubbles in oil," in *Proc. 7th Int. Conf. Prop. Appl. Dielectr. Mater.*, Nagoya, Japan, Jun. 2003, pp. 1120–1123.

[14] J. Li, Q. Hu, X. Zhao, X. Yao, Y. Luo, and Y. Li, "Partial-discharge characteristics of free spherical conducting particles under AC condition in transformer oils," *IEEE Trans. Power Del.*, vol. 26, no. 2, pp. 538–546, Apr. 2011.

[15] R. Sarathi, A. J. Reid, and M. D. Judd, "Partial discharge study in transformer oil due to particle movement under DC voltage using the UHF technique," *Electr. Power Syst. Res.*, vol. 78, no. 11, pp. 1819–1825, Nov. 2008.

[16] J. Tang, Y. Zhang, C. Pan, R. Zhuo, D. Wang, and X. Li, "Impact of oil velocity on partial discharge characteristics induced by bubbles in transformer oil," *IEEE Trans. Dielectr. Electr. Insul.*, vol. 25, no. 5, pp. 1605–1613, Oct. 2018.

[17] J. Tang, S. Ma, X. Li, Y. Zhang, C. Pan, and J. Su, "Impact of velocity on partial discharge characteristics of moving metal particles in transformer oil using UHF technique," *IEEE Trans. Dielectr. Electr. Insul.*, vol. 23, no. 4, pp. 2207–2212, Aug. 2016.

[18] S. Li, B. Gao, and G. Wu, "Influences of oil flow speed and temperature on partial discharge properties in transformer oil," in *Proc. Australas. Univ. Power Eng. Conf.*, Brisbane, QLD, Australia, Sep. 2016, pp. 1–4.

[19] *Effect of Particles on Transformer Dielectric Strength, in CIGRE Working Group 17 of Study Committee 12*, Paris, France, CIGRE, 2000.

[20] S. Jayaram, "Effects of thermal and viscous drag forces on AC breakdown characteristics of transformer oil," in *Proc. IEEE Conf. Elect. Insul. Dielectr. Phenom.*, Pocono Manor, PA, USA, Oct. 1993, pp. 396–401.

[21] *High-voltage Test Techniques: Partial Discharge Measurements*, Standard IEC-60270, 2000.

[22] *Insulating Liquids-Determination of the Breakdown Voltage at Power Frequency-Test Method*, Standard IEC-60156, 2018.

[23] C. Pan, J. Tang, Y. Zhang, X. Luo, and X. Li, "Variation of discharge characteristics with temperature in moving transformer oil contaminated by metallic particles," *IEEE Access*, vol. 6, pp. 40050–40058, 2018.

[24] M. M. Góngora-Nieto, P. D. Pedrow, B. G. Swanson, and G. V. Barbosa-Cánovasa, "Impact of air bubbles in a dielectric liquid when subjected to high field strengths," *Innov. Food Sci. Emerg. Technol.*, vol. 4, no. 1, pp. 57–67, Mar. 2003.

[25] H. Yamashita and H. Amano, "Prebreakdown density change, current and light emission in transformer oil under non-uniform field," *J. Electrost.*, vol. 12, pp. 253–263, Apr. 1982.

[26] V. Armenio and V. Fiorotto, "The importance of the forces acting on particles in turbulent flows," *Phys. Fluids*, vol. 13, no. 8, pp. 2437–2440, Aug. 2001.

[27] S. Birlasekaran, "The measurement of charge on single particles in transformer oil," *IEEE Trans. Electr. Insul.*, vol. 26, no. 6, pp. 1094–1103, Dec. 1991.

[28] N. N. Levedev, "Force acting on conducting sphere in the field of a parallel plate condenser," *Sov. Phys. Tech. Phys.*, vol. 7, pp. 268–270, Jan. 1962.

[29] X. Wang, Z. D. Wang, and J. Noakhes, "Motion of conductive particles and the effect on AC breakdown strengths of esters," in *Proc. IEEE Int. Conf. Dielectr. Liq.*, Trondheim, Norway, Jun. 2011, pp. 1–4.

[30] *Insulating Liquids-Determination of the Partial Discharge Inception Voltage (PDIV)-Test Procedure*, Standard IEC 61294, 1993.

[31] M. D. Judd, L. Yang, and I. B. B. Hunter, "Partial discharge monitoring of power transformers using UHF sensors. Part I: Sensors and signal interpretation," *IEEE Electr. Insul. Mag.*, vol. 21, no. 2, pp. 5–14, Mar./Apr. 2005.

[32] R. Sarathi, A. V. Giridhar, and K. Sethupathi, "Analysis of partial discharge activity by a conducting particle in liquid nitrogen under AC voltages adopting UHF technique," *Cryogenics*, vol. 50, no. 1, pp. 43–49, Jan. 2010.

[33] E. Husain and R. S. Nema, "Analysis of paschen curves for air, N2 and SF6 using the townsend breakdown equation," *IEEE Trans. Electr. Insul.*, vol. EI-17, no. 4, pp. 350–353, Aug. 1982.

[34] H. Okubo, N. Hayakawa, and A. Matsushita, "The relationship between partial discharge current pulse waveforms and physical mechanisms," *IEEE Electr. Insul. Mag.*, vol. 18, no. 3, pp. 38–45, May/Jun. 2002.

[35] A. Pedersen, G. C. Crichton, and I. W. McAllister, "The theory and measurement of partial discharge transients," *IEEE Trans. Electr. Insul.*, vol. 26, no. 3, pp. 487–497, Jun. 1991.

[36] S. Birlasekaran and M. Darveniza, "Microdischarges from particles in transformer oil," *IEEE Trans. Electr. Insul.*, vol. EI-11, no. 4, pp. 162–163, Dec. 1976.

[37] L. Dascalescu, M. Mihailescu, and R. Tobazeon, "Modeling of conductive particle behavior in insulating fluids affected by DC electric fields," *IEEE Trans. Ind. Appl.*, vol. 34, no. 1, pp. 66–74, Jan./Feb. 1998.

[38] Z. Liu, Q. Liu, and Z. D. Wang, "Effect of electric field configuration on streamer and partial discharge phenomena in a hydrocarbon insulating liquid under AC stress," *J. Phys. D, Appl. Phys.*, vol. 49, no. 18, Apr. 2016, Art. no. 185501.

[39] T. M. P. Briels, J. Kos, G. J. J. Winands, E. M. van Veldhuizen, and U. Ebert, "Positive and negative streamers in ambient air: Measuring diameter, velocity and dissipated energy," *J. Phys. D, Appl. Phys.*, vol. 41, no. 23, Nov. 2008, Art. no. 234004.

[40] D. J. Swaffield, P. L. Lewin, G. Chen, and S. G. Swingler, "Partial discharge characterization of streamers in liquid nitrogen under applied AC voltages," *IEEE Trans. Dielectr. Electr. Insul.*, vol. 15, no. 3, pp. 635–646, Jun. 2008.

[41] O. Lesaint and R. Tobazeon, "Streamer generation and propagation in transformer oil under AC divergent field conditions," *IEEE Trans. Electr. Insul.*, vol. 23, no. 6, pp. 941–954, Dec. 1988.

YONGZE ZHANG was born in Tai'an, Shandong, China, in 1988. He received the bachelor's degree from Southwest Jiaotong University. He is currently pursuing the Ph.D. degree with the State Key Laboratory of Power Transmission Equipment and System Security, Chongqing University, China. His research interests include partial discharge mechanism and high-voltage electric equipment insulation online monitoring.

JU TANG was born in Pengxi, Sichuan, China, in 1960. He received the bachelor's degree from Xi'an Jiaotong University and the master's and Ph.D. degrees from Chongqing University.

He is currently a Professor with the State Key Laboratory of Power Transmission Equipment and System Security, Chongqing University, and also with Wuhan University. His current research interests include high-voltage electric equipment insulation online monitoring and fault diagnosis.

CHENG PAN (S'12–M'17) was born in Guangshui, China, in 1986. He received the B.S. and Ph.D. degrees in electrical engineering from Xi'an Jiaotong University, China, in 2008 and 2014, respectively. Then, he joined State Grid Corporation of China as a Transformer Engineer. In 2015, he became a Lecturer at Wuhan University, China, and held a postdoctoral position. His research interests include partial discharge mechanism, surface charge accumulation at dc voltage, and breakdown characteristics of moving transformer oil.

XINYU LUO was born in Chongqing, China, in 1991. He received the bachelor's degree from Chongqing University, China, where he is currently pursuing the Ph.D. degree. His research interests include high-voltage electric equipment insulation online monitoring and fault diagnosis.